Advances in Optoacoustic Neurotomography of Animal Models

Article *in* Trends in Biotechnology · October 2019

DOI: 10.1016/j.tibtech.2019.07.012

3 authors, including:

Saak V. Ovsepian
National Institute of Mental Health
132 PUBLICATIONS **1,986** CITATIONS

SEE PROFILE

Please cite this article in press as: Ovsepian et al., Advances in Optoacoustic Neurotomography of Animal Models, Trends in Biotechnology (2019), https://doi.org/10.1016/j.tibtech.2019.07.012

Review

Advances in Optoacoustic Neurotomography of Animal Models

Saak V. Ovsepian,[1,2,3,4,5,*] Ivan Olefir,[1,2] and Vasilis Ntziachristos[1,2,6,*]

Unlike traditional optical methods, optoacoustic imaging is less sensitive to scattering of ballistic photons, so it is capable of high-resolution interrogation at a greater depth. By integrating video-rate visualization with multiplexing and sensing a range of endogenous and exogenous chromophores, optoacoustic imaging has matured into a versatile noninvasive investigation modality with rapidly expanding use in biomedical research. We review the principal features of the technology and discuss recent advances it has enabled in structural, functional, and molecular neuroimaging in small-animal models. In extending the boundaries of noninvasive observation beyond the reach of customary photonic methods, the latest developments in optoacoustics have substantially advanced neuroimaging inquiry, with promising implications for basic and translational studies.

Highlights

Optoacoustic imaging combines optical contrast and acoustic resolution to surpass the diffraction barrier of high-resolution optical imaging.

Excellent penetration with specificity and scalability rendered optoacoustic imaging a promising modality for biomedical interrogation.

A wide range of neuroimaging applications enabled considerable advances in basic and translational optoacoustic studies in animal models and in humans.

Along with advances and opportunities, numerous limitations have also emerged, which are currently a matter of intense research.

Combined with evolving technologies, major developments are expected in noninvasive optoacoustic neuroimaging, facilitating the discovery process.

Surpassing Diffraction Barriers of Optical Imaging

Elucidating the fundamental relationship between the structure and function of living organisms is one of the principal objectives of contemporary bioscience. Historically, in biological and medical studies, structure was viewed and interrogated independently from function, with attempts at relating them limited to wishful thinking or speculative conjectures [1,2]. Since the times of Leeuwenhoek, light microscopy has been the main workhorse of structural interrogation, facilitating biological observation via steady magnification and meticulous description of organizational details. Two key limitations of light microscopy, however, imposed major obstacles on the relation of structural data to the functions of living systems [3,4]. First, high-resolution imaging of biological specimens typically came with fixation: that is, with a death sentence. Second, no matter how advanced the optical imaging tools are, explicit observations have always been constrained to the surface of the specimen, due to the scattering of ballistic photons in deep tissue, with detrimental effects on image formation. In optical imaging, the depth limit is set by the mean propagation distance for a photon before directionality loss, a feature termed as the **transport mean free path (TMFP)** (see Glossary), which in biological specimens is ~1 mm [3,5]. No existing high-resolution optical imaging modality can penetrate beyond this barrier, where the vast majority of biological processes unfold.

Optoacoustic (photoacoustic) imaging is an emerging hybrid interrogation modality. Through the combined effects of the optical contrast mechanism and acoustic resolution, optoacoustic imaging surpasses the diffraction barrier, penetrating deeper into the specimen [6,7]. It capitalizes on the photoacoustic effect induced by the irradiation of an absorber with a short (1–100 ns) laser pulse at 5–50 kHz, which on excitation converts the energy of photons into heat, causing a fast local temperature rise. The pressure fronts induced by the resultant thermoelastic expansion propagate as ultrasound (US) waves, which can be detected by broadband transducers (in the 1–100-MHz range) placed outside the specimen (Box 1). Based on these signals, an image is formed, through resolving their source and arrival time. Due to two to three orders of magnitude less scattering of US waves in biological specimens compared with photons, optoacoustic imaging achieves better spatial resolution in deep tissue. Remarkably, by a tradeoff between spatial resolution and penetration depth, all of the advantageous features of optoacoustic interrogation can be faultlessly scaled for microscopic, mesoscopic, and macroscopic applications.

In recent years, optoacoustic imaging has reached a great degree of maturity, enabling considerable progress in structural, functional, and molecular studies [8–10]. In this pursuit, two major technological breakthroughs are of particular importance. First, rapid sequential illumination of the tissue with

[1]Institute for Biological and Medical Imaging, Helmholtz Zentrum Munich, German Research Center for Environmental Health, Ingolstaedter Landstrasse 1, 85764 Neuherberg, Germany

[2]School of Bioengineering, Technical University of Munich, 81675 Munich, Germany

[3]Department of Experimental Neurobiology, National Institute of Mental Health, Topolová 748, 250 67 Klecany, Czech Republic

[4]Third Faculty of Medicine, Charles University, 116 36 Prague, Czech Republic

[5]Website: http://www.nudz.cz/en/

[6]Website: https://www.helmholtz-muenchen.de/ibmi/index.html

*Correspondence: saak.ovsepian@gmail.com, vntziachristos@tum.de

Please cite this article in press as: Ovsepian et al., Advances in Optoacoustic Neurotomography of Animal Models, Trends in Biotechnology (2019), https://doi.org/10.1016/j.tibtech.2019.07.012

Box 1. Photoacoustic Effect and Operational Principles of Optoacoustic Imaging

Optoacoustic imaging capitalizes on the generation of US waves following light absorption by molecules. To achieve this effect, pulsed or periodically modulated light is used. In biomedical imaging, the method detects US waves produced by endogenous chromophores or exogenous reporters in response to NIR light. On light absorption, molecules produce local heat, which induces pressure waves measured using microphones or piezoelectric sensors placed around the specimen (Figure I). Because sound propagation in scattering tissue is orders of magnitude better than photons, optoacoustic imaging achieves better spatial resolution in deep tissue than the customary optical imaging. The molecular specificity and excellent penetration depth of optoacoustic imaging have already proved useful for a wide range of medical and biological applications.

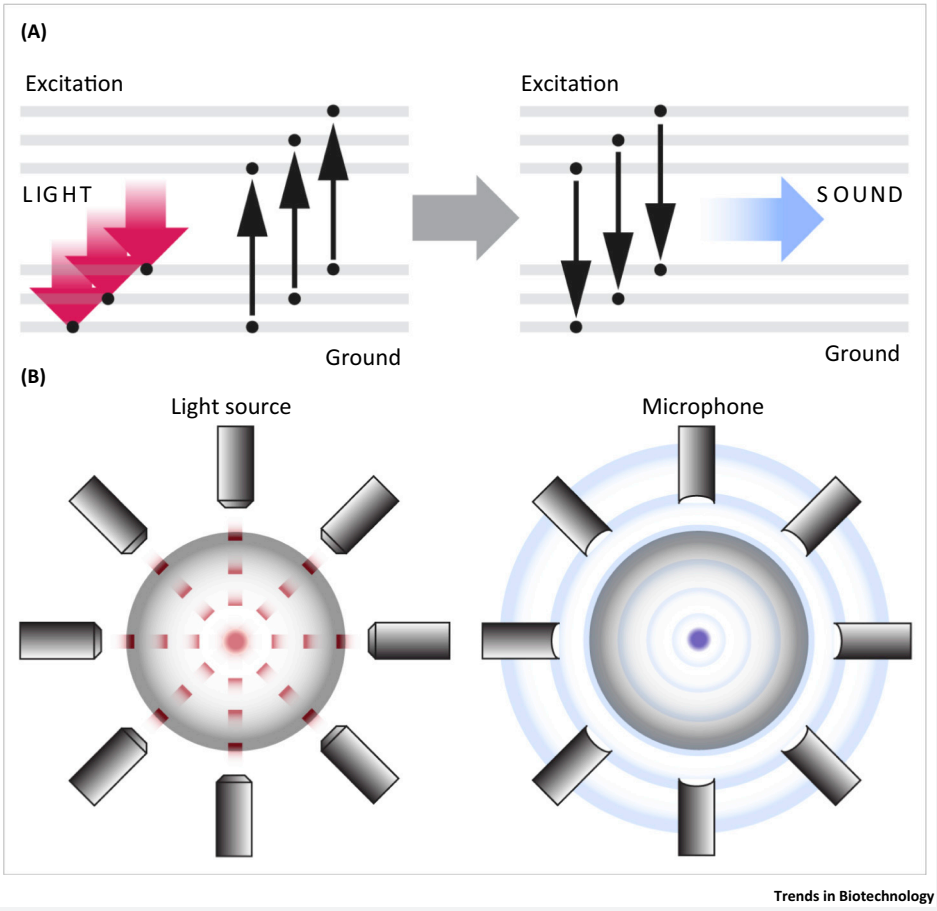

Figure I. Schematic of the Photoacoustic Effect and Its Applications.

(A) A schematic representation of the photoacoustic effect. Light absorption converts molecules from their ground to the excited state, which is followed by a return to the more stable ground state and energy release, partly in the form of molecular vibrations, generating ultrasound (US) waves. (B) The use of this principle for imaging applications.

multiple wavelengths and spectral unmixing makes it possible to simultaneously harness a wealth of spectral information from different absorbers. Second, by implementing advanced illumination and detection schemes, true volumetric observation is possible with a diffuse light, generating signals from the entire illuminated volume. In this review, we discuss recent advances in optoacoustic technologies and their neuroimaging applications in basic and translational studies in small-animal models.

Glossary

Acoustic impedance: a measure of the opposition that a system presents to the acoustic flow resulting from an acoustic pressure applied to the system.
Angiogenesis: the physiological process of formation of new blood vessels.
APP-PS1: transgenic mouse line expressing mutated amyloid precursor protein (APP) and presenilin-1 (PS1) mimicking amyloid plaque pathology of Alzheimer's disease.
Chromophores: a family of molecules that absorb particular wavelengths and in doing so confer color on the material.
Demyelination disease: neurological conditions resulting in damage to the protective covering (myelin sheath) that surrounds nerve fibers in the brain, optic nerves, and spinal cord.
Diffuse optical tomography (DOT): noninvasive imaging technique that utilizes light in the NIR spectral region to measure the optical properties of tissue.
Diffuse tensor imaging (DTI): MRI-based neuroimaging technique that makes it possible to estimate the location, orientation, and anisotropy of white matter tracts in the brain.
Di-R tracer: a NIR fluorescent carbocyanine die used for tracing neuronal tracts.
Electroencephalography (EEG): a neurophysiological method for monitoring the electrical activity of the brain.
Fluorescence multispectral tomography (FMT): an imaging modality mapping the distribution of molecules based on fluorescence properties.
Functional MRI (fMRI): an imaging modality used for measuring changes in blood flow related to brain activity.
Glioblastoma: the most aggressive form of brain cancer.
Hb and HbO_2: deoxy- and oxyhemoglobin; different states of the main blood chromophore Hb.
HuC-GCaMP5G: a vector expressing calcium-sensitive GCaMP5 under the HuC promoter encoding an RNA-binding protein implicated in neurogenesis.

Please cite this article in press as: Ovsepian et al., Advances in Optoacoustic Neurotomography of Animal Models, Trends in Biotechnology (2019), https://doi.org/10.1016/j.tibtech.2019.07.012

Scales and Dimensions of Optoacoustic Interrogation

As an inherently scalable method, optoacoustic imaging enables visualization at macroscopic, mesoscopic, and microscopic scales [7,9,11]. In neuroimaging, each of these scales is of key relevance to addressing specific sets of questions, ranging from noninvasive whole-brain interrogation at acoustic resolution to the visualization of cellular and subcellular processes at optical resolution [12,13]. On the macroscopic scale, optoacoustic imaging uses US detectors of ~5 MHz, which enable imaging at depths of several centimeters, with ~100–400 μm resolution [14,15]. On the mesoscopic scale, US detection in a frequency range of 10–100 MHz is used to achieve ~30–100 μm lateral resolution, with penetration, however, limited to a few millimeters. Finally, optoacoustic microscopy (OAM) uses focused laser beams for illumination, which can afford submicron diffraction-limited resolution, with penetration equivalent to optical microscopy (Figure 1A–F). Unlike single-element scanning techniques used for microscale imaging, in typical implementations optoacoustic mesoscopy and macroscopy utilize transducer arrays to capture pressure waves from the entire region of interest illuminated by a diffuse light source [16,17]. Through the use of model-based or back-projection reconstruction algorithms, high-resolution volumetric images are subsequently produced. For the majority of brain study applications, circular (or semicircular) or plane (cup) transducer arrays are used, which enable volumetric neuroimaging of rodents as well as larger animals such as dogs, sheep, and monkeys and, potentially, the human brain [12,18,19].

Multidimensionality is another advantageous feature of optoacoustic imaging. The term 'dimensionality' in this context has been extended to include, in addition to the traditional three geometrical dimensions, the time axis, the absorption wavelengths and the US frequency [9,12]. In most applications, acoustic lenses or curved detection arrays are applied to acquire 2D data, with the third dimension produced by the time delay of the optoacoustic signal, which is proportional to the speed of sound. The longer the delay, the deeper lies the source of the signal in the specimen. With diffuse illumination, a true volumetric interrogation is achieved, with captured signals translated into images based on time-resolved pressure waves. Using advanced excitation and sensing schemes, parallel detection of up to 512 channels at sampling rates of up to 125 MHz has been shown to be feasible, enabling video-rate tomographic imaging [20–22]. These developments are especially relevant for multidimensional mapping of neural functions at ultrafast timescales, with the added value of reduced motion artifacts.

The ability to resolve simultaneously multiple **chromophores** based on their absorption is perhaps the most valuable asset of optoacoustic imaging. Unlike mapping by **ultrasonography** of the **acoustic impedance** mismatch between various soft tissues, optoacoustic imaging resolves a wide range of molecular contrasts and absorbers, including endogenous chromophores such as hemoglobin, melanin, and cytochromes, as well as a range of other molecules, including lipid, water, ferratin, lipofuscin, and flavor proteins. With spectral unmixing, multiple series of images can be produced during a single imaging session, each representing the biodistribution of specific molecular contrasts with unique spectral signatures [8,23,24]. Utilizing high-speed **multispectral optoacoustic tomography (MSOT)**, up to 100 volumetric frames per second has been achieved [21], with even faster acquisition frame rates predicted to be within reach [9]. The development of specialized algorithms for motion correction and spectral unmixing should enhance multidimensional functional neuroimaging and correlation with structural information.

Multispectral Structural Optoacoustic Neuroimaging

Structural **magnetic resonance imaging (MRI)** represents a gold standard for noninvasive neuroanatomical studies, while MRI-based **diffuse tensor imaging (DTI)** is the main modality for fiber tracking and the study of long-range connections between different parts of the brain [25,26]. Although affording excellent penetration, these methods require special infrastructure and costly magnetic fields and operate at low spatial and temporal resolution [27,28]. Smaller brain size in experimental murine models imposes further constraints on structural MRI due to the disruptive effects of the skull on the magnetic field. Optical methods for deep tissue imaging such as **two-photon microscopy (TPM)** and **diffuse optical tomography (DOT)**, by contrast, afford excellent

Indocyanine green (ICG): a cyanine dye used in medical diagnostics and imaging.
iRFP: a NIR fluorescent protein used for labeling biological specimens for imaging and diagnostic purposes.
Ischemia: an inadequate blood supply to an organ or part of the body.
Isosbestic point: in spectroscopy, a specific wavelength at which the total absorbance of a sample does not change during a chemical reaction or a physical change of the sample.
Magnetic resonance imaging (MRI): a powerful biomedical interrogation method for noninvasive observation.
Multispectral optoacoustic tomography (MSOT): an emerging modality of optoacoustic imaging utilized for molecular imaging based on absorption spectra.
Near-IR (NIR): a region of the infrared spectrum of light used for spectroscopy (800–1680 nm).
Optical coherence tomography (OCT): an imaging technique that uses low-coherence light to capture micrometer-resolution images from within optical scattering media.
Phytochrome: a class of photoreceptor in plants, bacteria, and fungi used to detect light.
sO_2: the fraction of *oxygen-saturated* hemoglobin relative to total hemoglobin in the blood.
Transport mean free path (TMFP): the mean propagation distance for a photon before directionality loss.
Two-photon microscopy (TPM): a modality of high-resolution fluorescence imaging that allows the viewing of a living tissue up to about 1 mm depth.
Ultrasonography: a diagnostic imaging technique based on the application of US.
Xenografts: transplants of living cells, tissues, or organs from one species to another for research purposes.

Please cite this article in press as: Ovsepian et al., Advances in Optoacoustic Neurotomography of Animal Models, Trends in Biotechnology (2019), https://doi.org/10.1016/j.tibtech.2019.07.012

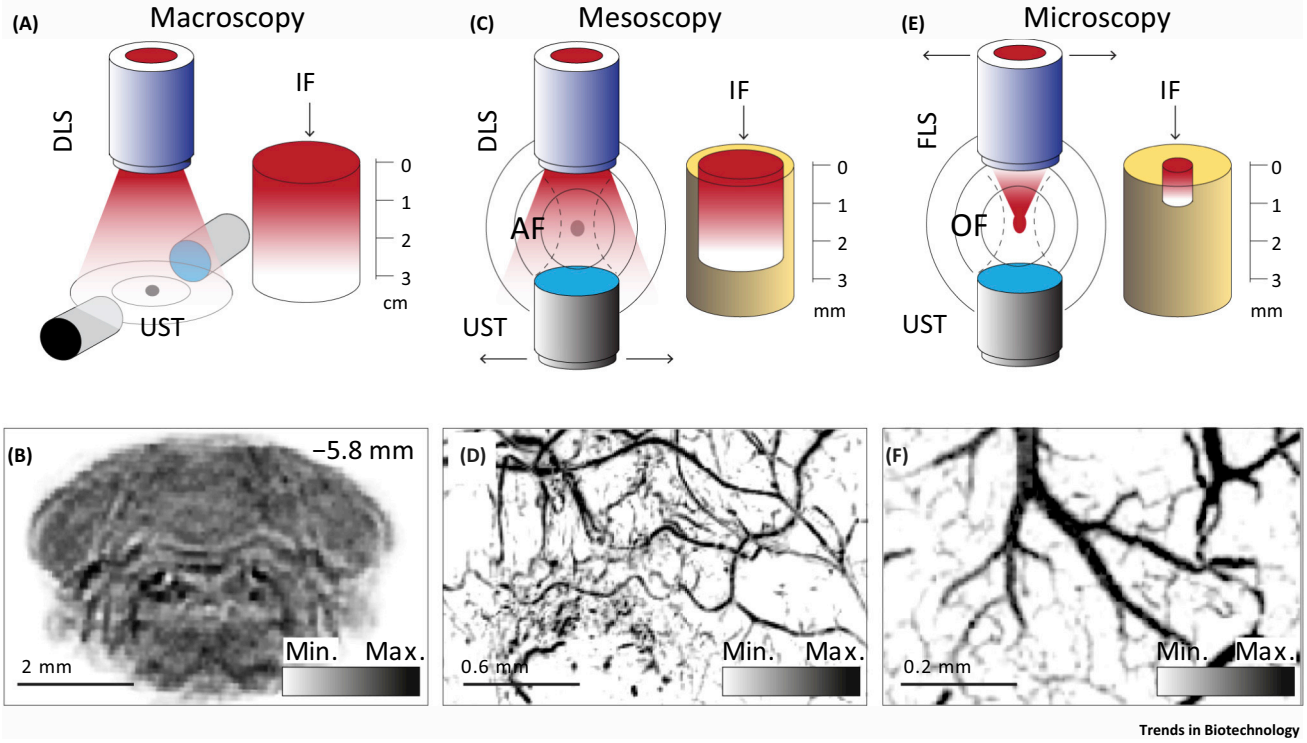

Figure 1. Schematic Illustration of the Relationship between the Spatial Resolution and Penetration Depth of Various Modalities of Optoacoustic Imaging.

Three interrogation modalities with representative images are shown. (A,B) Macroscopy, (C,D) mesoscopy, and (E,F) microscopy. (B,D,F) illustrate label-free images of coronal cross-section of the mouse cerebellum captured with multispectral optoacoustic tomography (MSOT) *ex vivo* (B), subcutaneous tumor vasculature in mouse model acquired with RSOM *in vivo* (D), and microvessel image acquired in the visual cortex of mouse *in vivo* (F). (B,D) Reproduced, with permission, from [12]; (F) modified from [71]. Abbreviations: DLS, diffuse light source; FLS, focused light source; AF, acoustic focus; OF, optical focus; IF, imaging field; UST, ultrasound transducer.

temporal resolution at lower cost but show limited penetration [29–31]. Also, in the majority of neuroimaging applications, two-photon imaging requires contrast enhancement using reporter proteins or fluorescent dyes.

Through conversion of the energy of diffuse light into US, optoacoustic imaging breaks the penetration barrier of optical imaging (~1 mm depth), enabling deeper interrogation across multiple scales at high resolution and lower cost compared with other modalities of biomedical imaging [6,10] (Table 1). With the added value of multispectral capabilities, it has been applied in a range of structural neuroimaging studies as well as in the comparative analysis of morphological changes associated with brain disease in intact- and open-skull murine preparations [12,13]. The majority of noninvasive structural studies capitalized on hemoglobin absorption [15,23,32–34]. Using external illumination, high-resolution brain cross-sections were obtained, revealing organization with exquisite anatomical detail (Figure 2A,B). In mice, numerous structural references in the brain were readily visualized using a transcranial approach [14,15,23,32,34]. In combination with ultrasonography in the same preparation, hybrid images were acquired and correlated with histological data [15]. By applying internal illumination through the oral cavity, high-resolution images of the ventral facet of the rat brain were also captured, revealing fine details of the basal vascular systems of the brain, the anterior and internal carotid arteries, and several major formations such as the hypothalamus and olfactory lobes, as well as the brain stem and optic nerve [33]. Importantly, both the molecular absorption and the anatomical contrast can be readily enhanced by the administration of exogenous agents such as **indocyanine green (ICG)** or by direct injection of **near-IR (NIR)**-liposome-AuNR into the brain,

Please cite this article in press as: Ovsepian et al., Advances in Optoacoustic Neurotomography of Animal Models, Trends in Biotechnology (2019), https://doi.org/10.1016/j.tibtech.2019.07.012

Modality	Resolution (μm)	Penetration (depth)	Sensitivity (molar)	Toxicity	Cost
OAM	<1	Low	Pico	High	Very low
TPM[b]	<1	Low	Pico	Medium	High
CFM[c]	<1	Very high	Pico	High	High
MSOT[d]	~20	Medium	Nano	Very low	Very low
MRI	~20	Very low	Nano	Very low	Very high
XCT	~50	Very low	Micro	Very high	Very high
US	~50	High	Pico	Very low	Very low

Table 1. Comparison of the Performance of the Optoacoustic Imaging with Other Major Biological Imaging Modalities[a]

[a]Adapted, with permission, from [12].
[b]TPM, two-photon microscopy.
[c]CFM, confocal microscopy.
[d]Multispectral optoacoustic tomography

improving the content of images [23,35,36]. Using the NIR **Di-R tracer**, the feasibility of MSOT-guided intracranial tracer injection and ventricular system mapping of the mouse brain has been also shown [34].

To determine the relative contributions of different endogenous chromophores in the formation of anatomical images, and to define the attenuating effects of the skull on the optoacoustic signal, brain images have been acquired before and after the removal of temporal bones or after perfusion and extraction of the brain from the cranium [12,14,34]. The fine structure of various brain parts could be observed in great detail with partial removal of skull bones [14]. It was shown that in the visible spectral range, cytochromes b and c play an essential role in the formation of anatomical images. Extending this analysis over the NIR range, unprecedented structural details of superficial and deep formations were revealed *in vivo* and *ex vivo* [12,34] (Figure 2A,B). These findings suggest that the differential distribution of lipids, proteins, and water throughout the brain plays a highly constructive role in image formation and the enhancement of anatomical content. Together with reports showing a constructive role for lipid in the formation of optoacoustic images of peripheral nerves *ex vivo* [37,38], these reports verify the utility of optoacoustics for mapping myelinated tracts in the central nervous system, with implications for neurodevelopment and **demyelination disease** studies. Another area of major relevance to structural neuroimaging is visualization of brain nuclei enriched with dark chromophores such as neuromelanin and neuroferritin [12,34]. Using MSOT with spectral unmixing in *ex vivo* brain images, the dopaminergic substantia nigra and ventral tegmental region have been visualized in mouse models, validating the potential suitability of MSOT for anatomical and developmental studies.

Large-Scale Functional Optoacoustic Neurotomography

Current understanding of brain mechanisms is largely based on electrophysiological data from selectively sampled neurons, often in partial or complete isolation. While offering excellent temporal resolution, noninvasive intra-vital neurophysiological methods fall short in assigning readouts to specific neuron types and functional processes [39]. The latter is very important given that dynamic assemblies of selected self-organizing neurons underlie a wide range of functions [40–42]. The inherent scalability and ability to monitor dynamic processes makes optoacoustic imaging compatible for mapping a wide range of functions of the intact brain.

In most functional studies, optoacoustic imaging was applied to capture activity-dependent changes in hemoglobin gradients and tissue perfusion [12,13]. Like **functional MRI (fMRI)**, label-free functional optoacoustics is capable of detecting changes in local blood-oxygen level-dependent signal contrast

Please cite this article in press as: Ovsepian et al., Advances in Optoacoustic Neurotomography of Animal Models, Trends in Biotechnology (2019), https://doi.org/10.1016/j.tibtech.2019.07.012

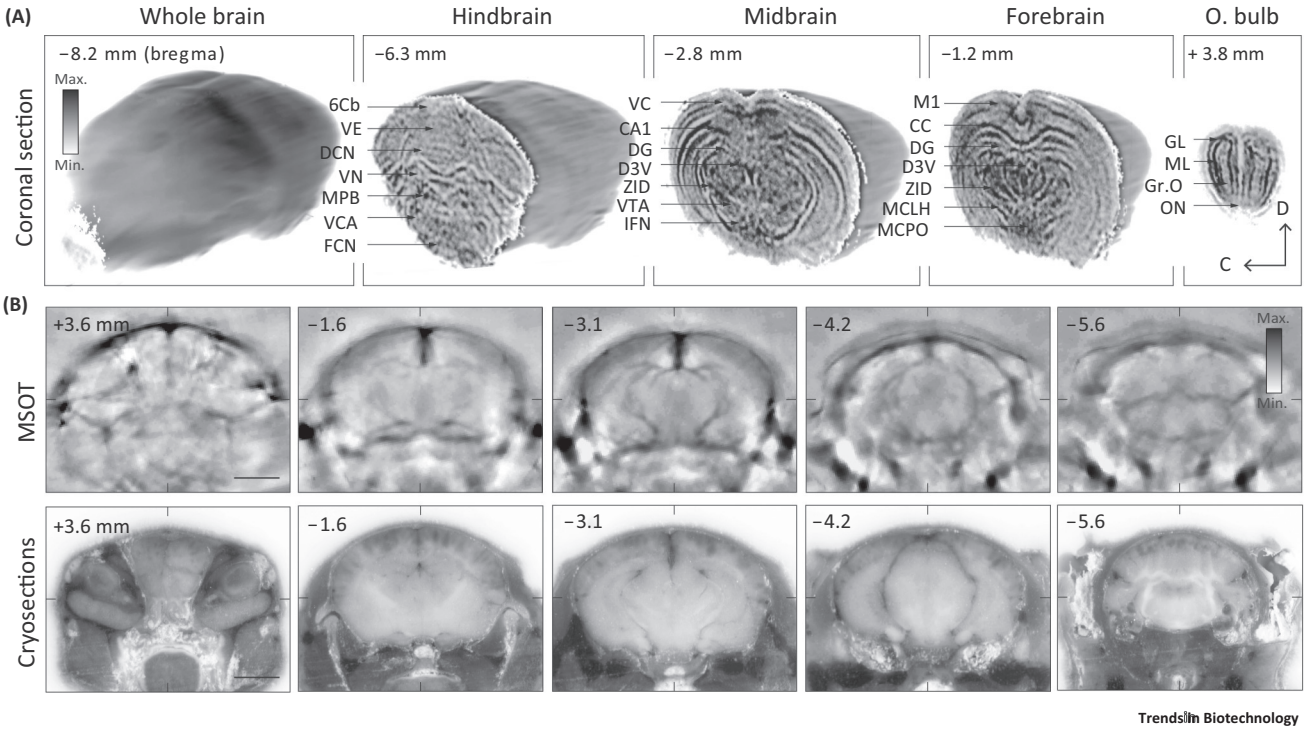

Figure 2. Label-Free Anatomical Multispectral Optoacoustic Tomography (MSOT) of Intact Mouse Brain *Ex Vivo* and *In Vivo*.

(A) Series of cross-sections at four different anatomical planes. (B) Series of consecutive MSOT cross-sections acquired *in vivo* (average of ten frames) and corresponding low-power images of the same brain captured on the cryoslicer. Note numerous exquisite anatomical details revealed by MSOT at all anatomical planes and depths throughout the entire-brain cross-sections, with their close correspondence to those captured using a digital camera. Adapted, with permission, from [34]. Abbreviations: 6Cb, sixth cerebellar lobule; VE, vermis; DCN, deep cerebellar nucleus; VN, vestibular nuclear complex; MPB, medial parabrachial nucleus; VCA, ventral cochlear nucleus; FCN, facial nucleus; VC, visual cortex; CA1, hippocampal CA1 region; DG, dentate gyrus; D3V, dorsal third ventricle; ZID, zona incerta dorsalis; VTA, ventral tegmental area; IFN, interfascicular nucleus; M1, motor cortex; CC, corpus callosum; MCLH, magnocellular lateral hypothalamus; MCPO, magnocellular preoptic nucleus; GL, glomerular layer; ML, mitral cell layer; Gr.O, granule cell layer; ON, olfactory nerve; C, caudal; D, dorsal.

[12,43]. Unlike fMRI, however, optoacoustic imaging with spectral unmixing can readily decompose and quantify **Hb and HbO_2** as well as levels of oxygen saturation in tissue with unprecedented accuracy, without uncertainties related to fluctuations of blood volume [44–46]. Using a multispectral approach, it produces spatial and temporal maps of the oxygen saturation of brain tissue (**sO_2**) with unprecedented accuracy proportional to the number of wavelengths employed [47]. Burton and colleagues applied MSOT to analyze changes in Hb, HbO_2, and sO_2 on cross-sections of a mouse brain before and during breathing gas challenges [23]. With multispectral data acquisition and spectral unmixing, hemoglobin gradient changes were related to the oxygenation state of the brain, showing alterations in the hemoglobin signal in the superior sagittal sinus, posterior cerebral arteries, and other prominent vessels on the brain. Applying a similar approach, the on and off rates of HbO_2, Hb, and sO_2 in the mouse somatosensory cortex were defined in response to alterations of the levels of O_2 and CO_2 in the breathing gas [15]. These measurements were coregistered with anatomical images of corresponding planes captured with ultrasonography to show that, under anesthesia, the rates of hemoglobin gradient changes in the somatosensory cortex exceed those in major brain vessels, implying stronger coupling of the brain tissue oxygenation with the breathing state. Utilizing a different geometry but a similar paradigm, five independent parameters (i.e., blood oxygenation, total hemoglobin, cerebral blood volume, Hb, and HbO_2) were acquired in real time from intact mice [48].

Please cite this article in press as: Ovsepian et al., Advances in Optoacoustic Neurotomography of Animal Models, Trends in Biotechnology (2019), https://doi.org/10.1016/j.tibtech.2019.07.012

In addition to sensing changes in hemoglobin signals related to gas challenge, optoacoustic imaging is capable of mapping fluctuations in the oxygenation levels of brain tissue under rest and induced by the activation of sensory inputs. Localized variations in Hb, HbO_2, and sO_2 were reported in the cerebral cortex in response to stimulation of paws or whiskers or the activation of visual inputs [34,49–51], delineating central representations of sensory systems in anaesthetized and behaving rodents. In freely moving rats, using portable 3D optoacoustic observation, video-rate imaging was achieved for the reconstruction of activity-dependent hemodynamic maps, which allowed comparison of the evoked response in the primary visual cortex (V1) and related circuits [50,52]. Through mapping the oxygen saturation rates at two wavelengths (710 and 840 nm), the extent and dynamics of V1 activation were determined before and after a flash of light, locked in time with the stimulus and decaying back to the baseline level after the removal of the stimulus. Earlier, spontaneous changes in hemoglobin gradients have been presented in resting mice, reflecting the default-mode brain activity with underlying connectivity [53]. Using single-wavelength optoacoustic imaging at 532 nm, which corresponds to the **isosbestic point** of the hemoglobin, eight predominant functional fields and several subregions were distinguished in the neocortex at 150 μm in plane resolution, based on the temporal coherence of intrinsic activity. Both the response pattern and the extent of synchrony between various fields showed high sensitivity to hypoxia. Multispectral analysis of the hemodynamic response has been recently extended to the detection of neural activation and dynamics across the entire mouse brain in response to somatosensory inputs, elucidating the architecture and distribution of subcortical and cortical activity related to processing somatosensory whisker inputs [34] (Figure 3A–F).

Combining fast tunable lasers and a transgenic approach, another study achieved real-time imaging of neural processes across the entire brain of zebrafish [21]. In a **HuC-GCaMP5G** model expressing a Ca^{2+} sensor protein under the HuC neuron-specific promoter [54], the resting state and pharmacologically induced neuronal activity were reconstructed *in vivo* and *ex vivo*, with 100 volumetric frames collected per second across scalable fields of view in the range 50–1000 mm^3 at a spatial resolution of 35–200 μm. Optoacoustic data were correlated with Ca^{2+}-dependent changes in fluorescence signals, showing close temporal coherence. Careful selection of wavelength and transducers with super-resolution methods is expected to enable fast functional readouts at the cellular scale in the near future. With added value of detecting endogenous contrasts, complementary imaging of Ca^{2+} or voltage-sensitive dyes represents a highly attractive asset for the analysis of brain activity.

Multidimensional Optoacoustic Imaging of Brain Disease Models

The arrival of noninvasive interrogation tools not only facilitated research on the normal brain but also enhanced the analysis of disease processes. In small-animal models, optoacoustic imaging has proved useful in elucidating a range of neurological disorders and disease models. As in neuroanatomical and functional studies, the majority of reports have taken advantage of pathological changes in endogenous chromophores, especially hemoglobin and melanin, while others benefited from the use of exogenous contrast agents. Among disease models, reports of brain tumors, traumatic brain disorders, **ischemia**, seizures of various etiology, and neurodegenerative conditions have been of special interest [23,48,55–58].

Applying video-rate MSOT, changes of hemoglobin gradients related to the growth of tumor **xenografts** have been mapped in the mouse brain [23]. Spectral decomposition revealed localized hypoxia in the core of the lesions, with tumor-affected areas especially visible under an enhanced CO_2 concentration (10%) in the breathing gas. The same study characterized the biodistribution and kinetics of the perfusion and clearance of ICG in the mouse brain. In the same vein, **iRFP**-expressing **glioblastomas** grafted at different depths of the mouse brain were visualized noninvasively at ~100 μm resolution, with growth of the tumor monitored over several weeks [35]. The method showed excellent utility for studies of early and advanced tumors, with the accuracy of readouts verified using **fluorescence multispectral tomography (FMT)** and X-ray CT (XCT) *in vivo*, followed by histology. Importantly, in comparative studies MSOT proved superior to FMT and XCT in resolving glioblastoma xerographs in deep brain compartments. Alterations of hemoglobin gradients with an increase in αvβ3

Please cite this article in press as: Ovsepian et al., Advances in Optoacoustic Neurotomography of Animal Models, Trends in Biotechnology (2019), https://doi.org/10.1016/j.tibtech.2019.07.012

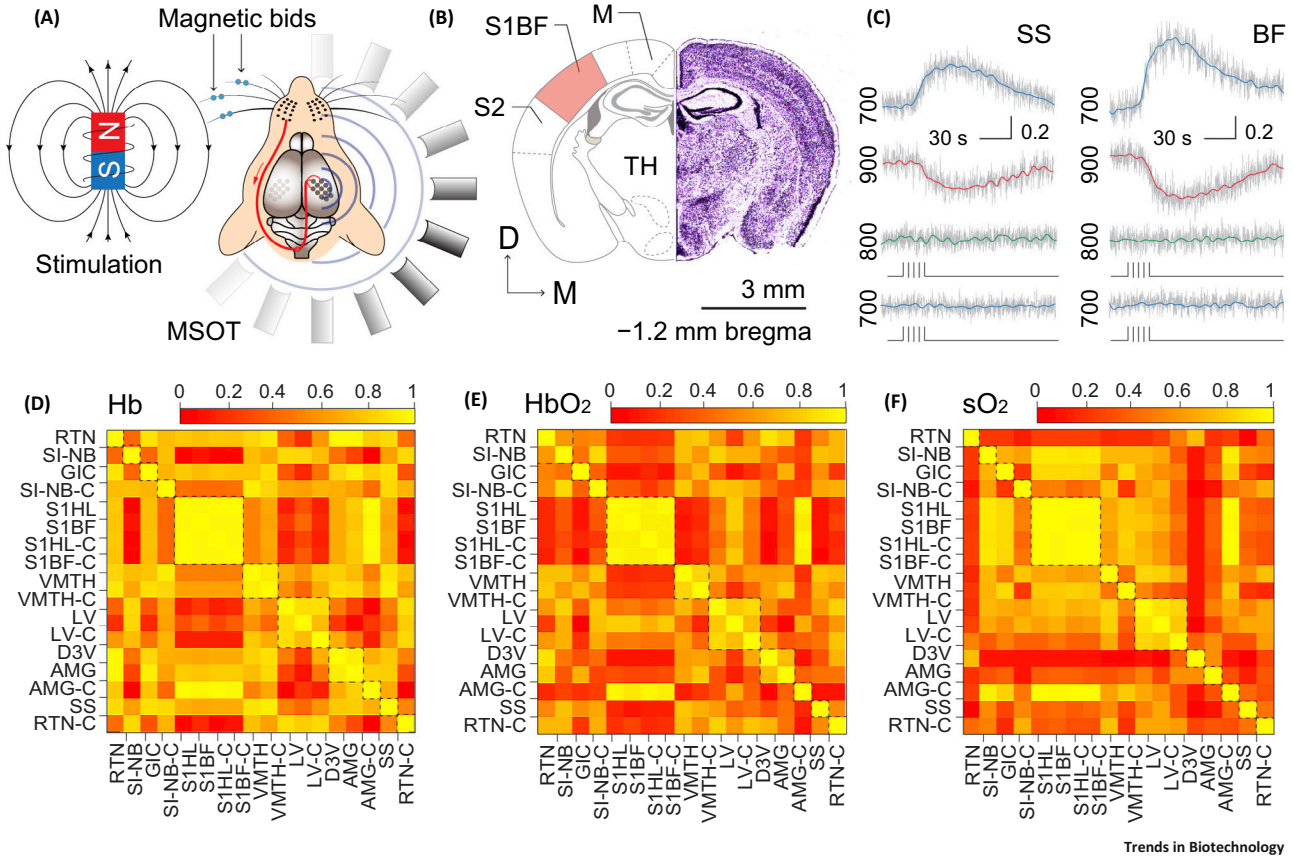

Figure 3. Functional Imaging of Large-Scale Neural Activity Using Multispectral Optoacoustic Tomography (MSOT).
(A) Schematic of the experimental design of whisker stimulation with pull–push magnet and setup for brain imaging with MSOT. (B) Mouse brain cross-section containing anatomical references such as somatosensory barrel cortex (S1BF), S2 somatosensory field (S2), and motor cortex (M) (left), with Nissl-stained brain slice of corresponding plane (right). (C) Typical traces of HbO_2 (900 nm), Hb (700 nm), and isosbestic (800 nm) signal acquired from experimental group (top) and HbO_2 and Hb signals from negative control group verifying that changes in Hb and HbO_2 are specific to activation of whisker inputs. (D–F) Cross-correlation matrix of Hb, HbO_2, and ${}_sO_2$ illustrating the degree of temporal coherence in the neurovascular response in different brain regions induced by activation of whisker inputs. The extent of correlation is shown in the color bar above each matrix, ranging from 0 to 1. The data are collected across entire-brain cross-sections containing the somatosensory barrel field and related structures. Details of experimental procedures and the significance of these measurements are provided in [34], from where the graphs are adapted with permission. Abbreviations: D, dorsal; M, medial.

integrin receptor expression and **angiogenesis** have been also detected. Decreased oxygen saturation in tumor implants suggested enhanced metabolism with hypoxia, a key hallmark of advanced cancer [56]. In the same vein, switchable **phytochrome** BphP1 was applied for brain tumor studies [59] (Figure 4A,B). Based on red-shifted absorption of BphP1 with photoconvertibility, both the location and the dimensions of xenografts were determined at ~100 μm resolution. The dynamic nature of the BphP1 signal yielded a greater signal-to-noise ratio with higher sensitivity than traditional contrast agents. In visualizing tumors, a tyrosine expression system has also shown major promise for optoacoustic imaging, with enrichment of melanin in nonmelanogenic tumors yielding excellent contrast [60].

Hb gradient changes have also proven useful for imaging brain strokes and ischemia *in vivo*. Deficit of tissue perfusion with widespread hypoxia caused by occlusion of the middle cerebral artery was used for longitudinal analysis of the functional dynamics in the affected area of living mice [55]. Extensive transient ischemia was induced in one hemisphere, with follow-up whole-brain MSOT demonstrating

Please cite this article in press as: Ovsepian et al., Advances in Optoacoustic Neurotomography of Animal Models, Trends in Biotechnology (2019), https://doi.org/10.1016/j.tibtech.2019.07.012

a dramatic drop in oxygenation at the core of the affected area with the surrounding tissue showing moderately reduced blood perfusion. Other reports applied occlusion of small arteries to investigate the impact of focal ischemia on **EEG** and hemodynamic changes induced by forepaw stimulation [49,61]. Under these conditions, a considerable drop in HbO_2 in the microvessel system downstream of the ablated arteries with compensatory adaptations has also been detected with the use of optical-resolution OAM [62]. Overall, these reports demonstrate a consistent decrease in hemoglobin signal with the decline of perfusion in ischemic regions, particularly prominent in cortical structures. Drug-induced seizures is another area of research where monitoring and mapping of hemoglobin dynamics with optoacoustic methods have proved instructive [12]. Video-rate volumetric imaging of the initiation and propagation of epileptic activity was implemented recently in mice with intracranial injection of the proconvulsive drug 4-aminopyridine (4-AP) [63]. Analysis of the hemoglobin gradients and EEG showed that the 4-AP injection site corresponds with the primary loci of generation of seizures, from where the hyperactivity propagated over the frontal lobe and in the thalamic nuclei. With a similar approach, bicuculline-induced seizures were mapped in the rat cerebral cortex [64,65]. In

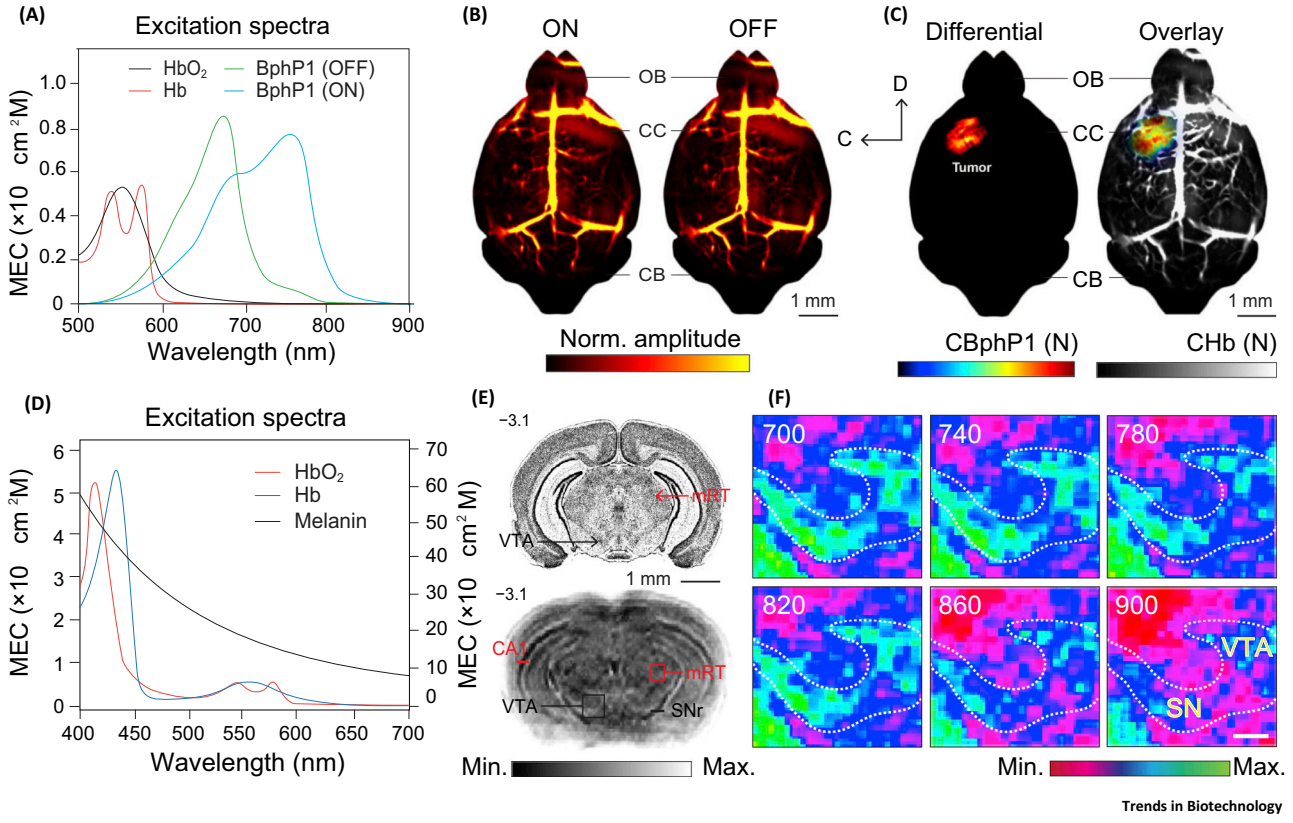

Figure 4. Imaging Brain Disease Models with Optoacoustic Tomography.

(A) Characterization of optical and acoustic properties of the nonfluorescent bacterial phytochrome BphP1. Molar extinction spectra of oxyhemoglobin (HbO_2), deoxyhemoglobin (Hb), BphP1 (ON), and BphP1 (OFF) are shown. (B,C) The ON and OFF state optoacoustic image of nude-mouse brain *in vivo* acquired 2 weeks after grafting of BphP1-expressing U87 tumor cells ~3 mm under the surface. The tumor is invisible in both the ON and the OFF state, due to overwhelming background signals from the blood (B). The differential image, by contrast, shows the tumor by suppressing background signals from the blood (C). Adapted, with permission, from [59]. (D) Excitation spectra of oxyhemoglobin (HbO_2), deoxyhemoglobin (Hb), and melanin. (E) Images of mouse brain cross-sections in slices enhanced with Nissl staining (top) and corresponding anatomical plane cross-section with multispectral optoacoustic tomography (MSOT) from the *ex vivo* whole brain. (F) Zoomed-in MSOT images of substantia nigra and neighboring structures acquired at multiple wavelengths demonstrate wavelength-dependent absorption changes in the region corresponding to neuromelanin-rich dopaminergic nuclei. Adapted, with permission, from [34]. Abbreviations: OB, olfactory bulb; CC, cerebral cortex; CB, cerebellum; VTA, ventral tegmental area; CA1, hippocampal CA1 region; SNr, substantia nigra; nRT, reticular thalamic nucleus. -3.1, bregma coordinate.

Please cite this article in press as: Ovsepian et al., Advances in Optoacoustic Neurotomography of Animal Models, Trends in Biotechnology (2019), https://doi.org/10.1016/j.tibtech.2019.07.012

combination with depth-resolved **optical coherence tomography (OCT)**, microscopic resolution optoacoustic imaging was used to visualize cortical hyperactivity after injection of 4-AP, with monitoring of the localized microvascular response at seizure foci [64]. Simultaneous measurements from arteries and veins showed that both vessel types are strongly dilated in the core of epileptic activity.

In studies of neurodegenerative disease models, optoacoustic imaging proved useful for visualizing neuromelanin-rich dopaminergic neurons of the midbrain and brain stem on entire-brain cross-sections [34] and amyloid plaques through cranial opening in Congo red-injected **APP-PS1** Alzheimer's disease mice [66]. In terms of sensitivity and resolution, amyloid plaque imaging data with OAM are comparable to those obtained using two-photon microscopy, but showing greater penetration [67,68]. The potential utility of optoacoustic methods for noninvasive whole-brain imaging of Alzheimer's plaques remains to be shown. Recent advances in the development of NIR contrast agents (i.e., AOI-987, DANIR-2) for labeling amyloid fibrils [12,69,70] hold promise for further research in this direction. Visualization of brain nuclei enriched with endogenous chromophores such as neuromelanin and neuroferritin has been proved feasible [12,34] and could be used for studies of neurodegenerative conditions, particularly Parkinson's disease manifested by extensive loss of midbrain dopaminergic neurons.

Outstanding Questions

How can we enhance label-free structural and functional neuroimaging in intact animal models and in humans using optoacoustic methods?

Which parameters of light transport and spectral coloring most compromise optoacoustic data and how can they be corrected?

What are the most promising directions in developing contrast agents for optoacoustic imaging, to better visualize selected processes?

How can we minimize imaging artifacts and ensure a maximally accurate representation of multidimensional processes in the brain?

Concluding Remarks and Future Perspectives

The celebrated American baseball player Yogi Berra notes that 'one can observe a lot by just watching'. While acknowledging the fine heuristic power of visual inspection, this statement also attests to its limitations. In optical imaging, the boundaries of visual inspection are set by scattering and reflection of the incident light, limiting the observation to the surface of the specimen. Rapidly maturing optoacoustic imaging has pushed the frontiers of visual inspection deeper into the specimen, through the acquisition of broadband US signals emitted in response to light absorption from deep compartments of specimens. Using elaborate algorithms, the US signals are translated into a 3D image, exposing a wealth of structural features and functional processes. Despite recent progress, problems remain, demanding further research and optimization (see Outstanding Questions). Improving spectral unmixing and quantification of signals is one area undergoing intense research. Concepts and algorithms are being developed for modeling light transport and spectral coloring, to eliminate their effects on acquired data and to ensure accurate readouts with image reconstruction and quantification. Major challenges also remain in solving issues related to the attenuation and distortion of light and sound in biological specimens, due to complex interactions with tissues and especially with the skull. In this direction, new results are emerging through the use of cutting-edge technologies with improved light delivery and enhanced light and sound propagation. Investigations are also under way to meet the pressing need for new contrast agents with high photoacoustic conversion, which would enable the labeling of selected structures and processes with better physical and spectral characteristics, improved biocompatibility, and low toxicity. Finally, research is under way toward the clinical translation of optoacoustics to human brain imaging. Offering better temporal resolution than fMRI and spatial resolution and molecular specificity than US, optoacoustic tomography holds major promise as an emerging interrogation method to elucidate a wide range of neural mechanisms and cognitive phenomena. Despite major challenges due to the strong scattering of light and US by the human skin and skull, considerable progress has been made in improving the image quality and incident light delivery. Careful consideration of these and other issues combined with emerging technologies in optics, photonics, and biotechnology are expected to further enhance the noninvasive real-time observation of brain structure and function in animal models, and potentially in humans, to facilitate the discovery process and the clinical translation of optoacoustic methods.

Acknowledgments

The authors' research at the Institute for Biological and Medical Imaging is supported by the German Government and the EU (grants to V.N.) and a Helmholtz Association Developmental Grant (S.V.O.). S.V.O. was also supported by project Nr LO1611 from the Ministry of Education, Youth and Sport (MEYS) under the National Sustainability Plan (NPU I) program.

Please cite this article in press as: Ovsepian et al., Advances in Optoacoustic Neurotomography of Animal Models, Trends in Biotechnology (2019), https://doi.org/10.1016/j.tibtech.2019.07.012

References

1. Gould, S.J. (1974) The origin and function of "bizarre" structures: antler size and skull size in the "Irish elk", *Megaloceros giganteus*. *Evolution* 28, 191–220
2. Rupke, N.A. (2009) *Richard Owen: Biology without Darwin*, Revised edn, University of Chicago Press
3. Ntziachristos, V. (2010) Going deeper than microscopy: the optical imaging frontier in biology. *Nat. Methods* 7, 603–614
4. Wilt, B.A. *et al.* (2009) Advances in light microscopy for neuroscience. *Annu. Rev. Neurosci.* 32, 435–506
5. Gigan, S. (2017) Optical microscopy aims deep. *Nat. Photonics* 11, 14–16
6. Ntziachristos, V. *et al.* (2005) Looking and listening to light: the evolution of whole-body photonic imaging. *Nat. Biotechnol.* 23, 313–320
7. Wang, L.V. and Yao, J. (2016) A practical guide to photoacoustic tomography in the life sciences. *Nat. Methods* 13, 627–638
8. Razansky, D. *et al.* (2009) Multispectral opto-acoustic tomography of deep-seated fluorescent proteins *in vivo*. *Nat. Photonics* 3, 412–417
9. Taruttis, A. and Ntziachristos, V. (2015) Advances in real-time multispectral optoacoustic imaging and its applications. *Nat. Photonics* 9, 219–227
10. Wang, L.V. and Hu, S. (2012) Photoacoustic tomography: *in vivo* imaging from organelles to organs. *Science* 335, 1458–1462
11. Taruttis, A. *et al.* (2015) Mesoscopic and macroscopic optoacoustic imaging of cancer. *Cancer Res.* 75, 1548–1559
12. Ovsepian, S.V. *et al.* (2017) Pushing the boundaries of neuroimaging with optoacoustics. *Neuron* 96, 966–988
13. Yao, J. and Wang, L.V. (2014) Photoacoustic brain imaging: from microscopic to macroscopic scales. *Neurophotonics* 1, 1877516
14. Li, L. *et al.* (2016) Label-free photoacoustic tomography of whole mouse brain structures *ex vivo*. *Neurophotonics* 3, 035001
15. Olefir, I. *et al.* (2016) Hybrid multispectral optoacoustic and ultrasound tomography for morphological and physiological brain imaging. *J. Biomed. Opt.* 21, 86005
16. Chekkoury, A. *et al.* (2016) High-resolution multispectral optoacoustic tomography of the vascularization and constitutive hypoxemia of cancerous tumors. *Neoplasia* 18, 459–467
17. Soliman, D. *et al.* (2015) Combining microscopy with mesoscopy using optical and optoacoustic label-free modes. *Sci. Rep.* 5, 12902
18. Petrov, I.Y. *et al.* (2012) Optoacoustic monitoring of cerebral venous blood oxygenation though intact scalp in large animals. *Opt. Express* 20, 4159–4167
19. Nie, L.M. *et al.* (2012) Photoacoustic tomography through a whole adult human skull with a photon recycler. *J. Biomed. Opt.* 17, 110506
20. Buehler, A. *et al.* (2012) Three-dimensional optoacoustic tomography at video rate. *Opt. Express* 20, 22712–22719
21. Dean-Ben, X.L. *et al.* (2016) Functional optoacoustic neuro-tomography for scalable whole-brain monitoring of calcium indicators. *Light Sci. Appl.* 5, 16201
22. Gateau, J. *et al.* (2013) Ultra-wideband three-dimensional optoacoustic tomography. *Opt. Lett.* 38, 4671–4674
23. Burton, N.C. *et al.* (2013) Multispectral opto-acoustic tomography (MSOT) of the brain and glioblastoma characterization. *Neuroimage* 65, 522–528
24. Ntziachristos, V. and Razansky, D. (2010) Molecular imaging by means of multispectral optoacoustic tomography (MSOT). *Chem. Rev.* 110, 2783–2794
25. Buchbinder, B.R. (2016) Functional magnetic resonance imaging. *Handb. Clin. Neurol.* 135, 61–92
26. Mori, S. and Zhang, J. (2006) Principles of diffusion tensor imaging and its applications to basic neuroscience research. *Neuron* 51, 527–539
27. Ugurbil, K. *et al.* (2013) Pushing spatial and temporal resolution for functional and diffusion MRI in the Human Connectome Project. *Neuroimage* 80, 80–104
28. Le Bihan, D. (2003) Looking into the functional architecture of the brain with diffusion MRI. *Nat. Rev. Neurosci.* 4, 469–480
29. Helmchen, F. and Denk, W. (2005) Deep tissue two-photon microscopy. *Nat. Methods* 2, 932–940
30. Ji, N. *et al.* (2016) Technologies for imaging neural activity in large volumes. *Nat. Neurosci.* 19, 1154–1164
31. Boas, D.A. *et al.* (2004) Diffuse optical imaging of brain activation: approaches to optimizing image sensitivity, resolution, and accuracy. *Neuroimage* 23, S275–S288
32. Li, L. *et al.* (2017) Single-impulse panoramic photoacoustic computed tomography of small-animal whole-body dynamics at high spatiotemporal resolution. *Nat. Biomed. Eng.* 1, 0071
33. Lin, L. *et al.* (2015) *In vivo* deep brain imaging of rats using oral-cavity illuminated photoacoustic computed tomography. *J. Biomed. Opt.* 20, 016019
34. Olefir, I. *et al.* (2019) Spatial and spectral mapping and decomposition of neural dynamics and organization of the mouse brain with multispectral optoacoustic tomography. *Cell Rep.* 26, 2833–2846.e3
35. Deliolanis, N.C. *et al.* (2014) Deep-tissue reporter-gene imaging with fluorescence and optoacoustic tomography: a performance overview. *Mol. Imaging Biol.* 16, 652–660
36. Lozano, N. *et al.* (2012) Liposome–gold nanorod hybrids for high-resolution visualization deep in tissues. *J. Am. Chem. Soc.* 134, 13256–13258
37. Mari, J.M. *et al.* (2014) Multispectral photoacoustic imaging of nerves with a clinical ultrasound system. *Proc. SPIE* 8943, 8903W
38. Matthews, T.P. *et al.* (2014) Label-free photoacoustic microscopy of peripheral nerves. *J. Biomed. Opt.* 19, 16004
39. Yuste, R. (2015) From the neuron doctrine to neural networks. *Nat. Rev. Neurosci.* 16, 487–497
40. Buzsaki, G. (2010) Neural syntax: cell assemblies, synapsembles, and readers. *Neuron* 68, 362–385
41. Hummel, J.E. and Biederman, I. (1992) Dynamic binding in a neural network for shape recognition. *Psychol. Rev.* 99, 480–517
42. Mesulam, M.M. (1998) From sensation to cognition. *Brain* 121, 1013–1052
43. Ogawa, S. *et al.* (1990) Brain magnetic resonance imaging with contrast dependent on blood oxygenation. *Proc. Natl. Acad. Sci. U. S. A.* 87, 9868–9872
44. Laufer, J. *et al.* (2007) Quantitative spatially resolved measurement of tissue chromophore concentrations using photoacoustic spectroscopy: application to the measurement of blood oxygenation and haemoglobin concentration. *Phys. Med. Biol.* 52, 141–168
45. Laufer, J. *et al.* (2005) *In vitro* measurements of absolute blood oxygen saturation using pulsed near-infrared photoacoustic spectroscopy: accuracy and resolution. *Phys. Med. Biol.* 50, 4409–4428
46. Tzoumas, S. *et al.* (2016) Eigenspectra optoacoustic tomography achieves quantitative blood oxygenation imaging deep in tissues. *Nat. Commun.* 7, 12121
47. Tzoumas, S. *et al.* (2015) Effects of multispectral excitation on the sensitivity of molecular optoacoustic imaging. *J. Biophotonics* 8, 629–637

48. Gottschalk, S. *et al.* (2015) Noninvasive real-time visualization of multiple cerebral hemodynamic parameters in whole mouse brains using five-dimensional optoacoustic tomography. *J. Cereb. Blood Flow Metab.* 35, 531–535
49. Liao, L.D. *et al.* (2012) Transcranial imaging of functional cerebral hemodynamic changes in single blood vessels using *in vivo* photoacoustic microscopy. *J. Cereb. Blood Flow Metab.* 32, 938–951
50. Tang, J. *et al.* (2016) Wearable 3-D photoacoustic tomography for functional brain imaging in behaving rats. *Sci. Rep.* 6, 25470
51. Wang, X. *et al.* (2003) Noninvasive laser-induced photoacoustic tomography for structural and functional *in vivo* imaging of the brain. *Nat. Biotechnol.* 21, 803–806
52. Tang, J. *et al.* (2015) Noninvasive high-speed photoacoustic tomography of cerebral hemodynamics in awake-moving rats. *J. Cereb. Blood Flow Metab.* 35, 1224–1232
53. Nasiriavanaki, M. *et al.* (2014) High-resolution photoacoustic tomography of resting-state functional connectivity in the mouse brain. *Proc. Natl. Acad. Sci. U. S. A.* 111, 21–26
54. Akerboom, J. *et al.* (2012) Optimization of a GCaMP calcium indicator for neural activity imaging. *J. Neurosci.* 32, 13819–13840
55. Kneipp, M. *et al.* (2014) Functional real-time optoacoustic imaging of middle cerebral artery occlusion in mice. *PLoS One* 9, e96118
56. Li, M.L. *et al.* (2008) Simultaneous molecular and hypoxia imaging of brain tumors *in vivo* using spectroscopic photoacoustic tomography. *Proc. IEEE* 96, 481–489
57. Staley, J. *et al.* (2010) Growth of melanoma brain tumors monitored by photoacoustic microscopy. *J. Biomed. Opt.* 15, 040510
58. Tsytsarev, V. *et al.* (2012) *In vivo* imaging of epileptic activity using 2-NBDG, a fluorescent deoxyglucose analog. *J. Neurosci. Methods* 203, 136–140
59. Yao, J. *et al.* (2016) Multiscale photoacoustic tomography using reversibly switchable bacterial phytochrome as a near-infrared photochromic probe. *Nat. Methods* 13, 67–73
60. Paproski, R.J. *et al.* (2014) Multi-wavelength photoacoustic imaging of inducible tyrosinase reporter gene expression in xenograft tumors. *Sci. Rep.* 4, 5329
61. Liao, L.D. *et al.* (2013) Study of neurovascular coupling functions for transient focal cerebral ischemia in rat using electrocorticography functional photoacoustic microscopy (ECoGfPAM). In *Proceedings of the 2013 Annual International Conference of the IEEE Engineering in Medicine and Biology Society*, pp. 1799–1802, IEEE Engineering in Medicine and Biology Society
62. Hu, S. *et al.* (2011) Optical-resolution photoacoustic microscopy of ischemic stroke. *Proc. SPIE* 7899, 789906
63. Gottschalk, S. *et al.* (2017) Correlation between volumetric oxygenation responses and electrophysiology identifies deep thalamocortical activity during epileptic seizures. *Neurophotonics* 4, 011007
64. Tsytsarev, V. *et al.* (2013) Photoacoustic and optical coherence tomography of epilepsy with high temporal and spatial resolution and dual optical contrasts. *J. Neurosci. Methods* 216, 142–145
65. Zhang, Q. *et al.* (2008) Non-invasive imaging of epileptic seizures *in vivo* using photoacoustic tomography. *Phys. Med. Biol.* 53, 1921–1931
66. Hu, S. *et al.* (2009) Intravital imaging of amyloid plaques in a transgenic mouse model using optical-resolution photoacoustic microscopy. *Opt. Lett.* 34, 3899–3901
67. Hefendehl, J.K. *et al.* (2011) Long-term *in vivo* imaging of beta-amyloid plaque appearance and growth in a mouse model of cerebral beta-amyloidosis. *J. Neurosci.* 31, 624–629
68. Meyer-Luehmann, M. *et al.* (2008) Rapid appearance and local toxicity of amyloid-beta plaques in a mouse model of Alzheimer's disease. *Nature* 451, 720–724
69. Cui, M. *et al.* (2014) Smart near-infrared fluorescence probes with donor–acceptor structure for *in vivo* detection of beta-amyloid deposits. *J. Am. Chem. Soc.* 136, 3388–3394
70. Tong, H. *et al.* (2015) Near-infrared fluorescent probes for imaging of amyloid plaques in Alzheimer's disease. *Acta Pharm. Sin. B* 5, 25–33
71. Wang, L. *et al.* (2013) Single-cell label-free photoacoustic flowoxigraphy *in vivo*. *Proc. Natl. Acad. Sci. U. S. A.* 110, 5759–5764